

Molecular Structure and Self-Aggregation of Amphiphilic Star Block Copolymers in Solution

Loan Huynh, Chris Neale, Régis Pomès and Christine Allen

1. Introduction

Linear, amphiphilic diblock and triblock copolymers have emerged as the materials of choice for use in a wide range of biomedical applications, including fabrication or coating of biomedical devices, drug delivery, and tissue engineering.¹⁻⁴ The use or integration of block copolymers in these technology platforms brings unparalleled diversity since they can be synthesized such that they self-organize or self-assemble, under specific conditions, to form superstructures with dimensions on the order of the nano- or microscale.⁵ Self-organization of these materials into ordered structures is reliant on the presence of specific intra- or intermolecular interactions or forces. Understanding the relationship between the composition of these materials and the self-organized superstructures they form is necessary, and possibly sufficient, for their rational design and use in particular applications.

Recent advances in synthetic procedures have afforded controlled preparation of block copolymers having complex architectures, such as dendrimer-like, graft-block, or star-block copolymers (SCPs).⁶⁻⁸ The SCP(s) may be designed to form unimolecular or multimolecular micelles depending on the copolymer composition and architecture.⁹⁻¹¹ Of particular interest, unimolecular micelles are not faced with issues relating to thermodynamic instability and may be prepared to be smaller in size with a more narrow size distribution than most multimolecular systems.^{12,13} To date, numerous SCP systems have been put forth in an attempt to design unimolecular micelles. These SCPs include star amphiphilic block copolymers based on poly(ethylene glycol)-*b*-polycaprolactone (PEG-*b*-PCL) and PEG-*b*-poly(L-lactide).^{9,10} In only a few cases, however, have the solution properties of these systems been studied systematically. As such, there remains a limited understanding of the relationship between the composition and architecture of SCPs (such as the number of arms, the nature and length of hydrophobic/hydrophilic blocks and the total molecular weight), their self-organizing behavior, and the properties of the unimolecular or multimolecular micelles that they form. As well, few studies have examined the structure of the core, the hydration state of the core and corona-forming blocks, and the composition of the core-corona interface in SCP systems. These

parameters influence important properties of the micelles, such as thermodynamic and kinetic stability, degradation profile, and solute loading capacity.

Computational methods have recently been used to study the behaviour of SCP unimolecular and their multimolecular micelles.¹⁴⁻¹⁶ However, the solution behavior of these copolymers and their intermolecular interactions have not been previously explored with atomistic detail. This is likely due to the fact that significant computational resources are required for these large systems. The aim of this study is to gain fundamental insight into the properties of SCPs in aqueous solution by conducting atomistic molecular dynamics (MD) simulation studies of these systems in explicit water. The atomistic level of detail enables explicit treatment of the physical basis of molecular self-aggregation including the intermolecular interactions that underlie the hydrophobic effect.

In light of the potential benefits of monodisperse unimolecular micelles, attention is focused largely on parameters that are likely to influence the equilibrium governing copolymer self-aggregation and micelle disassembly, indirectly probing the mechanism of self-aggregation. The present study yields unprecedented insight into the conformations adopted by the SCPs as well as detailed information on the hydrophobic PCL and hydrophilic PEG blocks, and their interactions with water, during self-organization. This information has the potential to guide the design of the next generation of SCPs.

2. Methodology

2.1. Simulated Systems

The series of SCPs under investigation have six identical arms radiating from a small central core. The arms are composed of methoxyPEG (MePEG) and PCL (i.e. [MePEG_x-*b*-PCL_y]₆, Table 1). The twelve systems simulated contain a single hydrated [MePEG_x-*b*-PCL_y]₆ SCP and vary systematically in terms of the degree of polymerization of the PEG, N_{PEG}, and PCL, N_{PCL}, in each arm (i.e. number of repeat units, x and y, respectively) as well as in terms of total MW of the SCP and N_{PCL}:N_{PEG} ratio. The composition and size of each system used in the MD simulations is outlined in Table 1.

2.2. Star Block Copolymer Parameters

The parameters for Lennard-Jones interactions and Ryckaert-Bellemans dihedrals applied to the [MePEG_x-*b*-PCL_y]₆ SCPs were taken from the optimized potential for the liquid simulations (OPLS) parameter set.^{17,18} The parameters for the CH₂OCOOCH₂ fragment that connects PCL to PEG were adapted from those of dimethyl carbonate¹⁹ as outlined in Table 2. A complete list of SCP charge assignments is included in Table 3. The simple point charge (SPC) water model was used as explicit solvent.²⁰

2.3. Molecular Dynamics Simulation Protocol

The initial coordinates for the [MePEG_x-*b*-PCL_y]₆ SCPs were generated using Cerius² 4.6 software (Accelrys Inc., San Diego, CA.).²¹ MD simulations were performed using the leap-frog algorithm for integrating Newton's equations of motion²² with the GROMACS 3.3.1 simulation software.^{23,24} A cubic box containing water and one solute molecule was constructed with an initial minimum distance of 1.0 nm between the solute and the boundary. In all MD simulations, the particle-mesh Ewald (PME)^{25,26} method was used to calculate the electrostatic interactions every time step with a real-space cutoff of 0.9 nm. Lennard-Jones interactions were computed using the group-based twin-range cutoff method,²⁷ calculating interactions every step for separation distances less than 0.9 nm and every ten steps for separation distances less than 1.4 nm, when the nonbonded list was updated. The LINCS²⁸ algorithm was applied to constrain the bond length of the solute and the SETTLE²⁹ algorithm was applied to water molecules to constrain its internal geometry. MD simulation was then carried out without position restraints for 200 ns with an integration time step of 2 fs. The coordinates were stored every 10 ps. Following 5000 steps of steepest-descent energy minimization, a short MD simulation was performed in the NPT ensemble at a constant pressure of 1 bar and a temperature of 27°C, while applying position restraints to the solute. The pressure was controlled isotropically by a Berendsen barostat³⁰ with a coupling time constant of 4.0 ps⁻¹. To control the temperature, the solute and the solvent were separately coupled to Berendsen thermostats³⁰ with coupling constants of 0.1 ps⁻¹.

2.4. Analysis

Structure: Structural analyses were performed by utilizing analysis tools from GROMACS 4.0.1. The average radius of gyration for each hydrophobic PCL core,

R_{g_core} , was determined based on the total MW of the PCL blocks and the central connection, whereas the average radius of gyration of the hydrophilic PEG, R_{g_PEG} , was calculated based on the radius of gyration of each arm of the SCP. The asphericity index of the hydrophobic PCL core was determined according to the method described by Bruns and Carl³¹ (supplemental information) where the asphericity index is zero for a perfect sphere and approaches one as the degree of asphericity increases.

Hydration: The first hydration shell was determined based on the first minimum of the radius distribution function (RDF) of water around PEG (0.35 nm). The total number of water molecules within the first hydration shell of the six PEG arms excluding the six OCH₃ terminal groups, W_{PEG} , were calculated and then used to determine the average number of water molecules bound per PEG repeat unit (W_{per_PEG}). The solvent accessible surface area of the hydrophobic PCL core (SAS_{PCL}) and PEG blocks, excluding the six OCH₃ terminal groups, (SAS_{PEG}) for the SCPs in aqueous solution were evaluated using the algorithm of Connolly.³² Furthermore, the total surface area of the hydrophobic core (S_{PCL}) was calculated by assuming that PEG blocks provide absolutely zero coverage of the hydrophobic core. Therefore, the difference between S_{PCL} and SAS_{PCL} is the surface area of PCL that is protected by the PEG blocks ($S_{PEG-PCL}$). The average surface area of a water molecule in contact with the polymer, S_{H_2O} , was obtained from the $SAS_{PEG}:W_{PEG}$ ratio for the smallest simulation system. The S_{PCL} was then normalized with S_{H_2O} (0.102 nm²) in order to obtain the total number of water molecules able to access the surface of the hydrophobic core in the absence of PEG, W_{totPCL} .

3. Results

3.1. Structural Properties

Equilibration and convergence: The SCPs investigated in this study are composed of six MePEG-*b*-PCL arms covalently attached to a multifunctional initiator, as shown in Table 1. Snapshots of the conformation of [MePEG₁₁₃-*b*-PCL₁₈]₆ following 5 ns and 200 ns of simulation are shown in Figure 1a. The hydration and radius of gyration of [MePEG₁₁₃-*b*-PCL₁₈]₆ are shown in Figure 1b. According to these metrics, convergence of the simulation systems was obtained after 40 ns of MD simulation. Generally, during the MD simulations, the PCL blocks quickly collapse from a fully

extended conformation and form a compact core within 15 ns. The hydrophilic PEG blocks remain highly hydrated and assume disordered conformations with a high degree of structural heterogeneity.

Self-aggregated structure, size, and shape of PCL: The PCL blocks formed a compact hydrophobic core that excluded water and PEG. Concurrently, strong segregation occurred between the hydrophobic PCL core and the hydrophilic PEG corona, as shown in the spatial distribution function of [MePEG₁₁₃-*b*-PCL₁₈]₆ (Figure 2a). Importantly, self-organization of the hydrophobic PCL core was observed. The hydrophobic cores of SCPs with $N_{\text{PCL}} \geq 9$ (*i.e.* with $y = 9$ or 18) are relatively spherical, having an asphericity index of $\sim 0.008 \pm 0.001$. As N_{PCL} decreased, the shape of the hydrophobic core shifts towards an ellipsoid where the asphericity index of the core ranges from 0.02 to 0.05 as shown in Table 4. Amongst the different systems, the inner hydrophobic PCL core becomes more densely packed with increasing total MW_{PCL} and reaches a density of 1.1 to 1.2 $\text{g}\cdot\text{cm}^{-3}$ at a distance of 0.4 nm from the center of mass (COM) of the hydrophobic core (supplemental information).

As shown in Figure 3a, the average $R_{\text{g_core}}$ can be described as a function of N_{PCL} according to the following equation:

$$R_{\text{g_core}} = 0.605 (N_{\text{PCL}})^{0.275} \text{ (nm)}. \quad (1)$$

In addition, a linear relationship between the N_{PCL} and the volume of the hydrophobic core (V_{core} ; data not shown) was obtained and can be described by the following equation:

$$V_{\text{core}} = 1.44 N_{\text{PCL}} + 1.1 \text{ (nm}^3\text{)}. \quad (R^2 = 0.998) \quad (2)$$

Transition phase between PCL and PEG: There exists a distance from the COM of the core at which the density of PCL equals that of PEG, generally in the presence of a small but reproducible amount of water (Figure 2b). This represents the midpoint in the amphiphilic region or transition phase between the dominantly hydrophobic and hydrophilic regions of the aggregated copolymer. This phase begins

with the distal ends of the PCL blocks and the proximal ends of the PEG blocks and continues to the point where the density of the hydrophobic core approaches zero. Remarkably, for SCPs with $N_{\text{PCL}} \geq 3$, the thickness of this transition phase is $\sim 0.60 \pm 0.05$ nm independent of N_{PCL} and N_{PEG} with a maximum water density of 0.11 ± 0.02 g·cm⁻³ and maximum PCL or PEG densities of $\sim 0.50 \pm 0.02$ g·cm⁻³.

Conformation, size, and extension of PEG: In contrast to PCL, the PEG block is highly hydrated during the MD simulation, and thus the PEG corona is significantly less densely packed than the hydrophobic PCL core (see Figure 2b). As such, the PEG corona occupies a significantly larger volume than the core. For all SCPs investigated in the current study, the MD simulations reveal that the PEG blocks move rapidly and are globally disordered while transiently adopting a local helical structure with 3.5 PEG repeat units per turn. For SCPs with $N_{\text{PEG}} > 12$, the distal ends of the PEG blocks often extend away from the proximal ends, or curl back to form a Gaussian coil providing partial shielding of the hydrophobic core from solvent as shown in the time average distribution of the end-to-end distance (EED) of SCPs (supplemental Figure S2). For SCPs with shorter PEG chains, the ends of all PEG blocks remain extended, with a median EED of 0.80 ± 0.01 nm ($N_{\text{PEG}} = 6$) and 1.05 ± 0.01 nm ($N_{\text{PEG}} = 12$). The size of the PEG corona was determined based on the $R_{\text{g_PEG}}$. A linear relationship was obtained for $R_{\text{g_PEG}}$ plotted as a function of N_{PEG} (Figure 3b), allowing $R_{\text{g_PEG}}$ to be predicted using the following relationship:

$$R_{\text{g_PEG}} = 0.20 (N_{\text{PCL}})^{0.467} \text{ (nm)}. \quad (3)$$

3.2. Solvation Properties

Solvent accessible surface area and hydration of PCL: The total solvent accessible surface area of the hydrophobic PCL core in the absent of PEG, S_{PCL} , can be predicted according to Equation 4.

$$S_{\text{PCL}} = 0.58 \times 6 \times N_{\text{PCL}} + 11.36 \text{ (nm}^2\text{)} \quad (R^2 = 0.978) \quad (4)$$

As expected, S_{PCL} depends only on N_{PCL} , whereas, the solvent accessible surface area of PCL in the present of PEG (*i.e.* PEG partially protects PCL from water), SAS_{PCL} , is

significantly influenced by the PEG blocks such that an increase in N_{PEG} results in a decrease in SAS_{PCL} (Table 4).

MD simulation of SCPs in explicit water allowed the calculation of the number of water molecules in the first hydration shell (within 3.5 Å) of the polymers. A snapshot of the $[\text{MePEG}_{38}\text{-}b\text{-PCL}_9]_6$ SCP highlighting the interaction of the hydrophobic PCL core with water at a simulation time of 200 ns is shown in Figure 4a. Once the PCL component exceeds a total MW_{PCL} of 2.05 KDa ($N_{\text{PCL}} = 3$), the heart of the hydrophobic core is completely devoid of water. Importantly, the number of water molecules bound to the surface of the hydrophobic PCL core, W_{PCL} , was found to depend on both N_{PCL} and N_{PEG} . In particular, W_{PCL} decreased with an increase in N_{PEG} when N_{PCL} was held constant, as shown in Table 4. The quantification of this relationship is one of the major results in this study, and is an essential step towards the rational design of unimeric SCPs.

A linear relationship was obtained between N_{PCL} and W_{totPCL} , as shown in Figure 5a. The ratio of W_{PCL} to W_{totPCL} represents the fraction of the hydrophobic core exposed to water, f_{PCL} . Significantly, our results quantify the decrease in f_{PCL} with an increase in N_{PEG} (Figure 5b):

$$f_{\text{PCL}} = 1.0 - 0.126 \ln(6 \times N_{\text{PEG}}), \quad (5a)$$

$$\text{where } f_{\text{PCL}} = W_{\text{PCL}} / W_{\text{totPCL}}, \quad (5b)$$

$$\text{and } W_{\text{totPCL}} = 5.5 \times 6 \times N_{\text{PCL}} + 107. \quad (5c)$$

By substituting Equation 5(b-c) into Equation 5a, the W_{PCL} can be expressed as:

$$W_{\text{PCL}} = 33 \times N_{\text{PCL}} - 4.16 \ln(6 \times N_{\text{PEG}}) \times N_{\text{PCL}} - 13.5 \ln(6 \times N_{\text{PEG}}) + 107. \quad (6)$$

Solvent accessible surface area and hydration of PEG: The solvent accessible surface area of PEG, SAS_{PEG} , increases linearly with an increase in N_{PEG} (Table 5). This yields a theoretical description of SAS_{PEG} that can be expressed as:

$$\text{SAS}_{\text{PEG}} = 0.34 \times 6 \times N_{\text{PEG}} + 8.7 \text{ (nm}^2\text{)}. \quad (R^2 = 0.981) \quad (7)$$

For the various SCPs in this study, the SAS per PEG repeat unit ($\text{SAS}_{\text{per_PEG}}$) ranges from 0.36 to 0.57 nm². According to Equation 7, the average $\text{SAS}_{\text{per_PEG}}$ was independent of the PCL block length for all SCPs.

As shown in Table 5, large hydration values for PEG blocks were obtained for all SCPs, demonstrating a high solubility for PEG in water. The average number of water molecules predicted to bind per PEG repeat unit ranges from 3.2 to 5.4 for the various SCPs in this study (Table 5). Consistent with the SAS results for PEG, the average hydration number of PEG is proportional to N_{PEG} (Figure 5b):

$$W_{\text{PEG}} = 3.2 \times 6 \times N_{\text{PEG}} + 82 \text{ (molecules)}. \quad (8)$$

4. Discussion

4.1. Validation of Parameters for MD simulation: The current MD simulations reproduce the known aqueous properties of PCL and PEG blocks^{33,34}, wherein the hydrophobic PCL core is largely dehydrated and solvated by a water soluble PEG corona (Figure 2). Such fundamental properties emerge from these simulations in spite of the fact that the force fields that were employed do not contain any special terms, beyond partial charges, that directly control solubility (Table 2 and 3). Rather, hydrophobic collapse in these simulations is driven by the same forces that exist in a test tube, namely the entropically disfavoured formation of an aqueous solvation shell around a non-polar solute. This is consistent with the success of such a force field in computing the self-organization of other micelle-forming molecules, such as detergents, as well as the formation of lipid bilayers.^{35,36}

Structure and Dehydration of the PCL core: The aggregated structure of PCL that emerges from MD simulations agrees well with the known properties of this polymer (e.g. semi-crystalline and water insoluble), confirming that our simulations are sampling the relevant phase of this polymer. In particular, the PCL blocks form an ordered and compact hydrophobic core that excludes water and PEG (supplemental Figures). The linear relationship between $R_{\text{g_core}}$ and N_{PCL} for all simulated systems (Equation 1) indicates a similar packing pattern and architecture for PCL within the hydrophobic cores of all SCPs (Equation 1). This result is further supported by the linear relationship between V_{core} and N_{PCL} (Equation 2).

For $N_{\text{PCL}} \geq 4$, the partial overlap of the radial density of PCL and water that is apparent in Figure 2b is not the result of actual coexistence. Rather it is an artifact of the radial averaging of an inherently aspherical hydrophobic PCL core (Table 4). The same is true of PCL and PEG, which do not intermingle, beyond the close interactions of two rough interfaces. For $N_{\text{PCL}} \leq 3$, however, the exclusion of water from the PCL core is incomplete. In the current study, the present water found in the heart of the PCL core for $N_{\text{PCL}} \leq 3$, suggests that low MW_{PCL} degrades at a faster rate than high MW_{PCL} . Many studies have proposed that the presence of water at the PCL-PEG interface of micelles promotes hydrolytic degradation of the core (e.g. ester bond cleavage within the PCL blocks) of the polymers.³⁷ Further, an increase in the rate of degradation of PCL of decreasing MW has been reported based on dynamic light scattering (DLS), nuclear magnetic resonance and gel permeation chromatography measurements for $\text{MePEG}_x\text{-b-PCL}_y$ ($x = 117$, $y = 7, 13$ and 17) linear diblock copolymer micelles.³⁸

Hydration of the PEG corona: The present study provides a detailed measurement of hydration at the atomistic level with systematic exploration of polymer MW and conformation (Table 5 and Figure 5c). Equation 8 allows the prediction of the hydration of PEG of a known MW within the range of 0.3 KDa to 5.0 KDa, which encompasses the PEG polymers employed for numerous biomedical applications. These results are consistent with the known unlimited solubility of PEG in water³⁹⁻⁴¹ (Figure 5c) which has been suggested to be due to hydrogen bonding between the ether oxygen of the polymer and water.⁴² Furthermore, for SCPs with long PEG chains there is an increased probability that water molecules may form a hydrogen bonding “bridge” between PEG arms or PEG repeat units (supplemental Figure). Such water bridges have been found previously using ^1H and ^2H nuclear magnetic resonance measurements for PEG6000 in low water content.⁴³ In the current study, the decrease in $W_{\text{per_PEG}}$ values with an increase in N_{PEG} from 6 ($W_{\text{per_PEG}} = 5.4$) to 113 ($W_{\text{per_PEG}} = 3.2$) is indicative of the replacement of the water-PEG interactions by PEG-water-PEG and/or PEG-PEG interactions (Table 5).

As shown in Equation 8, the linear relationship for W_{PEG} as a function of N_{PEG} and the average $W_{\text{per_PEG}}$ obtained from the current study (3.2 to 5.4) are within the range of values determined experimentally for $W_{\text{per_PEG}}$ values (1.0 to 5.0).^{40,44-48} Specifically, Branca *et. al.* reported a linear relationship between the degree of hydration of PEG and MW_{PEG} ($N_{\text{PEG}} \sim 4.5$ to 45), with $W_{\text{per_PEG}}$ values ranging from 1.5 to 5.0 based on

viscosity measurements.⁴⁹ In another study, the minimum $W_{\text{per_PEG}}$ was found to be 2.5, as determined by measuring the heat capacity for the interaction between water and PEG8000 ($N_{\text{PEG}} = 182$).⁴¹ In comparison, a nuclear magnetic resonance spectroscopy study of PEG6000 by Lusse and Arnold suggested that there is a maximum of one water molecule in contact with a single PEG monomer unit.⁴³

As reviewed by Allen *et. al.*,³⁹ the variation in the number of water molecules reported to interact with a single PEG monomer unit may be attributed to differences in PEG conformation which depends largely on MW_{PEG} , architecture of the polymer and the environment (i.e. temperature, concentration, surface tethering, surface density). In this regard, Tirosch *et. al.* proposed that the conformations of PEG2000 grafted to liposomes and free in solution were brush ($W_{\text{per_PEG}} \sim 4.6$) and random coil ($W_{\text{per_PEG}} \sim 3.0$), respectively.⁴⁶ In another study, it was found that the degree of water uptake is dependent on the architecture of the SCP, such that increasing the number of arms resulted in a decrease in hydration as determined by gravimetric analysis of copolymer films.⁵⁰ Furthermore, the instruments used to measure the hydration of PEG can affect the hydration results. For example, the $W_{\text{per_PEG}}$ values ($N_{\text{PEG}} \sim 4.5$ to 45) obtained by acoustic measurements (1.5 to 5.0) were greater than those determined by viscosity measurements (2.0 to 3.5).⁴⁹ Importantly, the $W_{\text{per_PEG}}$ values obtained from the current study are direct measurements of water molecules that are in contact with the PEG blocks.

4.2. Relationship to other theoretical models

Previously, Flory put forth the “random flight” model to predict the size of linear polymers in terms of the radius of gyration.⁵¹ In the current study, the size of the PEG chain can be expressed in terms of the radius of gyration based on Flory’s theory, $R_{\text{gF_PEG}} = (a/\sqrt{6})N_{\text{PEG}}^\alpha$, where a is the size of one PEG repeat unit (supplemental information). As shown in Figure 3a, the linear fits from the plot of MW_{PEG} as function of radius of gyration on a double logarithmic scale yields α values of 0.467 for the PEG blocks in water (Equation 3). This result is similar to the α value for a theta solvent ($\alpha = 0.5$) in which the polymer is said to behave ideally and exist in a Gaussian coil.⁶² In comparison, the α value obtained for the PEG blocks from the current study is smaller than the

experimental α value obtained by DLS analysis of single-chain PEG in water (80 KDa < MW_{PEG} < 100 KDa), i.e. $\alpha = 0.583$,⁵² which is similar to the theoretical value for the polymer in good solvent ($\alpha = 0.588$, supplemental information). The discrepancy between MD simulation and experimental values for α may be attributed to the difference in MW. As shown in Table 5, the percent difference between the radii of gyration calculated based on Flory theory, R_{gF_PEG} , (supplemental information), and R_{g_PEG} obtained from the current study decreased with an increase in N_{PEG} (24 % to 11 %).

According to de Gennes' definition of random coil conformation, at a low graft density, the linear polymer adopts a random coil conformation in the “mushroom regime” which is defined as a “half-sphere with a radius comparable to the Flory radius, R_F , of a coil in a good solvent”.⁵³ Based on a model put forth by Torchilin and Papisov,⁵⁴ the surface area of PEG at the surface of PEGylated liposomes in water is proportional to the surface area of a hemisphere with a radius approximately equal to R_F , assuming a random coil conformation for the polymer.⁵³ Accordingly, the theoretical surface area of the PCL core protected by the PEG blocks was calculated to be equivalent to the following, $S_{\text{random-coil}} = \pi R_F^2$; where $R_F = aN^{3/5}$ (supplemental information).

From our results, the surface area of PCL protected from water by the PEG blocks, $S_{\text{PEG-PCL}}$, is dependent on both the PCL core size and the PEG length. In comparison to the $S_{\text{random-coil}}$, the $S_{\text{PEG-PCL}}$ values obtained from the current study were smaller with $N_{PEG} \leq 19$ and larger with $N_{PEG} \geq 27$ (Table 5). The discrepancy in values is mainly due to the approximate nature of the “half-spherical” assumption for the random coil model for PEG⁵³ (supplemental information), whereas the area of PCL protected by PEG determined from the MD simulations was calculated directly from the SAS of PEG and PCL blocks. Accordingly, the current study indicates that the volume occupied by the PEG blocks is relatively non-spherical prior to time averaging. Importantly, the brush and random coil model established by de Gennes⁵³ is unsuitable for describing the conformation of PEG in the current study. Thus, the theoretical model, established by Torchilin and Papisov⁵⁴ based on the random coil model for the calculation of the surface of hydrophobic area shielded by PEG, is not applicable for prediction of the required MW_{PEG} necessary to protect the PCL core from water.

4.3. Quantification of hydration of the PCL core as the thermodynamic basis for multimolecular aggregation

Although considerable effort has been expended both theoretically and experimentally to describe the effect of hydration on the macromolecular structure and stability of PEG-*b*-PCL micelles formed by SCPs or linear diblock copolymers^{34,40,44-48,55}, quantification of the number of water molecules that interact with PCL has remained elusive. For the first time we present a detailed molecular model quantifying the number of water molecules that interacts with the hydrophobic PCL core of various six-arm SCPs. Based on our analysis, the solvent accessible surface area of the hydrophobic PCL core depends not only on the surface area and aggregated structure of the copolymer, but also on the length and conformation of the PEG blocks, whereby increasing PEG block length reduces the exposure of the PCL core to the aqueous environment (Table 4). However, the W_{PCL} values presented in Table 4 demonstrate that none of the SCPs in this study contain a PEG corona that is capable of providing full coverage of the hydrophobic core, exposing segments of the PCL core to water.

In a concentrated aqueous solution of SCPs, the unshielded PCL units would also be in potential contact with PCL units of another unimer. The ability to predict the hydration of the hydrophobic PCL core is important in terms of self-aggregation. Specifically, we postulate that the propensity for aggregation of SCPs is correlated with the fractional hydration of the hydrophobic PCL core in the unimeric state, which was found to vary from 55% to 23% depending on the MW of the PCL and PEG blocks (Table 4, Figure 5a). Sufficient water exposed surface area of the non-polar PCL blocks may destabilize the unimeric state and thus drive intermolecular association between SCPs that result in the formation of multimolecular micelles in aqueous media. Accordingly, multimolecular micelles of SCPs with MW similar to [PEG₁₁₃-*b*-PCL₁₈]₆ were observed by DLS and transmission electron microscopy at a copolymer concentration of 3.4×10^{-6} mol/L in water (unpublished data). Significantly, the results of the present study are highly quantitative and, as such, may be utilized to rationally design a SCP with a hydrophobic core that is sufficiently protected from water such that it may exclusively form stable unimeric micelles.

4.4. Rational Design of Unimeric Micelles

Based on the present study, we propose that aggregation between SCPs is a result of interaction between water-exposed-PCL. The optimal ratio(s) of N_{PCL} to N_{PEG} of a SCP may be predicted to maximize the dehydration of the PCL core. In particular, extrapolation of Equation 6 for a known N_{PCL} illustrates the minimum N_{PEG} that is required to completely cover the PCL core. For example, $N_{\text{PCL}} = 18$ (MW = 2.6 KDa) requires $N_{\text{PEG}} = 464$ (MW = 20.4 KDa) in order to obtain $W_{\text{PCL}} \sim 0$. For this SCP (*i.e.* [MePEG₄₆₄-*b*-PCL₁₈]₆), the predicted $R_{\text{g_core}}$, V_{core} and $R_{\text{g_PEG}}$ are 1.34 nm, 27.0 nm³ and 3.52 nm obtained by extrapolating Equations 1, 2 and 3, respectively. Indeed PEG blocks of this MW have been employed to stabilize diblock copolymer micelle formulations.⁵⁶ In another study, 20 KDa PEG was conjugated to oncolytic adenovirus for intravenous injection into mice.⁵⁷ Further, for $N_{\text{PEG}} = 464$, the predicted $R_{\text{g_PEG}}$ (3.52 nm) extrapolated from Equation 3 is similar to the experimental $R_{\text{g_PEG}}$ of a 20 KDa PEG conjugated with fluorescent dye using DLS (experimental $R_{\text{g_PEG}} = 3.92 \pm 0.2$ nm) and fluorescence recovery after pattern photobleaching (experimental $R_{\text{g_PEG}} = 4.03 \pm 0.2$ nm).⁵⁸

It is important to emphasize that much of the information gained from the MD simulations cannot be obtained by performing experimental studies on the individual SCPs of the present study. Experimentally, these SCPs are likely to aggregate in solution, whereas our MD simulations sample the conformations adopted by unimers at infinite dilution, allowing us to fully characterize the unimeric state and identify the source of thermodynamic instability. The significance of the present study is the elucidation of quantitative relationships that are instrumental in the rational design of SCPs. The size of the SCP is more strongly related to N_{PEG} than to N_{PCL} (Table 5). And it is, in many cases, undesirable to increase the size of the unimeric micelle *ad infinitum* in order to achieve complete protection of the hydrophobic PCL core from solvent.

4.5. New SCP Architecture

The question remains whether PEG can completely protect the hydrophobic PCL core, since the water molecules that interact with PEG at the PEG-PCL interface can also interact with PCL. Regardless of PEG length, there is either a small amount of water interacting unfavourably with the hydrophobic core or a small amount of proximal PEG that is unfavourably dehydrated. Inclusion of an amphiphilic block between the hydrophobic and hydrophilic blocks may be desirable in some cases.

Furthermore, the architecture of the SCP may need to be modified in combination with optimization of the ratio of the PEG and PCL block lengths. As well, the chemical structure of the central connector may need to be considered in order to utilize the relationship between the structural properties and MW of the PCL core for other SCPs that have chemically-different connectors. It is worth noting that simply increasing the number of arms of the SCP may not necessarily result in a unimeric micelle. For example, a previous experimental study revealed that (MePEG₁₁₃-*b*-PCL₂₆)₁₆ SCPs formed multimolecular micelles (CMC of ca. 3 mg/mL).⁹ However, Schramm *et. al.* synthesized many SCPs having 4 and 6 arm PCL₁₂ cores ($N_{\text{PCL}} = 12$) that were conjugated to 4-, 6-, 8- and 12-branched-PEG ($N_{\text{PEG}} = 8$ to 30) per PCL arm.¹¹ Interestingly, these SCPs behave as unimolecular micelles according to DLS measurements.

5. Conclusions

Our simulations predict a densely packed hydrophobic core that is phase separated from a disordered and highly mobile hydrophilic PEG corona. The average number of water molecules predicted to bind per PEG repeat unit is in the range of 3.2 to 5.4. This result is in good agreement with experimental data for SCPs with high MW_{PEG}. The conformation of the hydrophobic PCL core and the conformational and solution properties of the PEG shell are predictable and independent of the ratio of hydrophilic to hydrophobic block length.

Although it is likely that a simple increase in the amount of PEG will be sufficient to entirely encapsulate the PCL core and protect the SCPs from PCL mediated aggregation, the MW of the SCP also needs to be considered for utilization of the material for a particular application (e.g. drug delivery). This report revealed that the PEG corona in many cases provides only partial coverage of the hydrophobic core, leaving segments of PCL exposed to water. Unique to this study, the hydration of the PCL core was quantified as a function of N_{PCL} and N_{PEG} enabling prediction of the minimum N_{PEG} required for complete protection of a core with a specific MW_{PCL}.

Acknowledgments

This study was supported by a grant from NSERC to C. Allen as well as a University of Toronto Open Fellowship to L. Huynh. C. Neale is funded by the Research Training Center at the Hospital for Sick Children and by the University of Toronto. The authors are grateful to the Centre for Computational Biology High Performance Facility (CCBHPPF) at the Hospital for Sick Children (Toronto, ON) and the Shared Hierarchical Academic Research Computing Network for generous allocations of computational resources (Toronto, ON). R. Pomès is a CRCP Chairholder. Thanks also to Fugang Li for synthesizing and characterizing the [MePEG₁₁₃-*b*-PCL₁₈]₆.

References:

1. Kumar N, Ravikumar MNV, Domb AJ 2001. Biodegradable block copolymers. *Adv Drug Deliv Rev* 53:23-44.
2. Allen CJ 2003. The Merging Fields of Polymer and Lipid-Based Drug Delivery (commentary). *J Liposome Research* 13:XI-XII.
3. Lavik E, Langer R 2004. *Appl Microbio and Biotech* 65:1-8.
4. Eberhart RC, Su SH, al. KTN 2003. *J of Biomat Sci - Polymer Edn* 14:299-312.
5. Forster S, Konrad MJ 2003. Star Polymers with Alternating Arms from Miktofunctional μ -Initiators Using Consecutive Atom Transfer Radical Polymerization and Ring-Opening Polymerization. *Materials Chemistry* 13:2671-2688.
6. Heise AH, J. L.; Frank, C. W.; Miller, R. D. 1999. *J Am Chem Soc* 121:8647.
7. Nguyen ABH, N.; Fetters, L. J. 1986. *Macromolecules* 19:768.
8. Mountrichas GM, M.; Pispas, S. 2005. *Macromolecules* 38:940.
9. Wang F, Bronich TK, Kabanov AV, Rauh RD, Roovers J 2005. Synthesis and evaluation of a star amphiphilic block copolymer from poly(ϵ -caprolactone) and poly(ethylene glycol) as a potential drug delivery carrier. *Bioconjugate Chem* 16:397.
10. Wang F, Bronich TK, Kabanov AV, Rauh RD, Roovers J 2008. Synthesis and Characterization of Star Poly(ϵ -caprolactone)-b-Poly(ethylene glycol) and Poly(L-lactide)-b-Poly(ethylene glycol) Copolymers: Evaluation as Drug Delivery Carriers. *Bioconjugate Chem*.
11. Schramm OG, Pavlov GM, Erp HPv, Meier MAR, Hoogenboom R, Schubert US 2009. A Versatile Approach to Unimolecular Water-Soluble Carriers: ATRP of PEGMA with Hydrophobic Star-Shaped Polymeric Core Molecules as an Alternative for PEGylation *Macromolecules* 42:1808-1816.
12. Jones M-C, Ranger M, Leroux J-C 2003. *Bioconjugate Chem* 14:774.
13. Liu M, Kono K, Frechet JMJ 2000. *J Controlled Rel* 65:121.
14. Xin J, Liu D, Zhong C 2007. Multicompartment Micelles from Star and Linear Triblock Copolymer Blends. *J Phys Chem B* 111:13675-13682.
15. Chang Y, Chen W-C, Sheng Y-J, Jiang S, Tsao H-K 2005. Intramolecular Janus Segregation of a Heteroarm Star Copolymer. *Macromolecules* 38:6201-6209.
16. Ganazzoli F, Y. A. Kuznetsov, Timoshenko EG 2001. Conformations of Amphiphilic Diblock Star Copolymers. *Macromol Theory Simul* 10:325-338.
17. Jorgensen WL OPLS, Force Field. *Encyclopedia of Computational Chemistry*, Vol. 3; Wiley: New York, 1998; pp 1986-1989.
18. Jorgensen WL, Maxwell DS, Tirado-Rives. J 1996. Development and Testing of the OPLS All-Atom Force Field on Conformational Energetics and Properties of Organic Liquids. *J Am Chem Soc* 118:11225 - 11236.
19. Okada O 1998. *Molecular Physics* 93:153-158.
20. Berendsen, H. J. C.; Postma, J. P. M.; van Gunsteren, W. F.; Hermans, J. Interaction Models for Water in Relation to Protein Hydration. In *Intermolecular Forces*; Pullman, B., Ed.; Reidel: Dordrecht, The Netherlands, 1981. ed.
21. Accelrys Software Inc., Cerius2 Simulation & Prediction, Release 4.6, San Diego: Accelrys Software Inc., 2001
22. Hockney RW, Goel SP, Eastwood J 1974. Quiet highresolution computer models of a plasma. *J Comp Phys* 14:148-158.
23. Berendsen HJC, Spoel Dvd, Drunen Rv 1995. GROMACS: A message-passing parallel molecular dynamics implementation. *Computer Physics Communications* 91:43 - 56.
24. Lindahl E, Hess B, Spoel Dvd 2001. GROMACS 3.0: a package for molecular simulation and trajectory analysis. *J Mol Mod* 7 306 - 317.

25. Darden T, York D, Pedersen L 1993. Particle mesh Ewald: An $N \cdot \log(N)$ method for Ewald sums in large systems. *J Chemical Phys* 98:10089 - 10092
26. Essmann U, Perera L, Berkowitz ML, Darden T, Lee H, L.G. Pedersen 1995. A smooth particle mesh ewald potential. *J Chem Phys* 103 8577-8592.
27. Gunsteren WFv, Berendsen HJC 1990. *Agnew Chem Int Ed Engl* 29 992.
28. Hess B, Bekker H, Berendsen HJC, Fraaije JGEM 1997. LINCS: A linear constraint solver for molecular simulations. *J Comput Chem* 18 1463-1472.
29. Miyamoto S, Kollman PA 1992. *J Comput Chem* 13:952.
30. Berendsen HJC, Postma JPM, Gunsteren WFv, Nola AD, Haak JR 1984. *J Chem Phys* 81:3684.
31. Bruns W, Carl W 1991. Relations between Averaged Configurational Properties of Linear and Starlike Polymer Models at the 8 Temperature. *Macromolecules* 24:209-212.
32. Connolly M 1983. Solvent-accessible surfaces of proteins and nucleic acids. *Science* 221:709-713.
33. Allen C, Yu Y, Maysinger D, Eisenberg A 1998. Polycaprolactone-b-poly(ethylene Oxide) Block Copolymer Micelles as a Novel Drug Delivery Vehicle for Neurotrophic Agents FK506 and L-685,818. *Bioconjugate Chem* 9:564-572.
34. Lu C, Liu L, Guo S-R, Zhang Y, Li Z, Gu J 2007. Micellization and gelation of aqueous solutions of star-shaped PEG-PCL block copolymers consisting of branched 4-arm poly(ethylene glycol) and polycaprolactone blocks. *Euro Polym J* 43:1857-1865.
35. Jorge M 2008. Molecular Dynamics Simulation of Self-Assembly of n-Decyltrimethylammonium Bromide Micelles. *Langmuir* 24:5714-5725.
36. Lensink MF, Loney C, Ruyschaert J-M, Vandenbranden M 2009. Characterization of the Cationic DiC14-amidine Bilayer by Mixed DMPC/DiC14-amidine Molecular Dynamics Simulations Shows an Interdigitated Nonlamellar Bilayer Phase. *Langmuir* 25:5230-5238.
37. Ha C-S, J. A. Gardella J 2005. Surface Chemistry of Biodegradable Polymers for Drug Delivery Systems. *Chem Rev* 105:4205-4232.
38. Shen C, Guo S, Lu C 2008. Degradation behaviors of monomethoxy poly(ethylene glycol)-b-poly(ϵ -caprolactone) nanoparticles in aqueous solution. *Polymers for Advanced Technologies* 19:66-72.
39. Allen C, Santos ND, Gallagher R, Chiu GNC, Shu Y, Li WM, Johnstone SA, Janoff AS, Mayer LD, Webb MS, Bally MB 2002. Controlling the Physical Behavior and Biological Performance of Liposome Formulations Through Use of Surface Grafted Poly(ethylene Glycol) *Bioscience Reports* 22:225-250.
40. Wenzel JG, Balaji KS, Koushik K, Navarre C, Duran SH, Rahe CH, Kompella UB 2002. Pluronic F127 gel formulations of deslorelin and GnRH reduce drug degradation and sustain drug release and effect in cattle. *J Control Release* 85:51-59.
41. Ng K, Rosenberg A 1990. Heat capacity of poly (ethylene glycol)-water mixtures: Poly (ethylene glycol)-water interactions. *Thermochimica Acta* 169 339-346.
42. Kjellander R, Florin EJ 1981. Water structure and changes in thermal stability of the system poly(ethylene oxide)-water. *Chem Soc Faraday Trans* 77:2053-2077.
43. Lusse S, Arnold K 1996. The interaction of poly(ethylene glycol) with water studied by H-1 and H-2 NMR relaxation time measurements. *Macromolecules* 29:4251-4527.
44. Lee JH, Lee HB, Andrade JD 1995. Blood compatibility of polyethylene oxide surfaces. *Prog Polym Sci* 20:1043-1079.
45. Elbert DL, Hubbell JA 1996. Surface treatments of polymers for biocompatibility. *Ann Rev Mat Sci* 26:365-394.

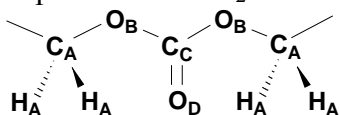
46. Tirosh O, Barenholz Y, Katzhendler J, Prieve A 1998 Hydration of Polyethylene Glycol-Grafted Liposomes. *Biophys J* 74 1371-1379.
47. Needham D, Hristova K, McIntosh TJ, Dewhirst M, Wu N, Lasic DD 1992. Polymer-grafted liposomes: physical basis for the “steal” property. *J Liposome Res* 2:411-430.
48. Needham D, McIntosh TJ, Lasic DD 1992. Repulsive interactions and mechanical stability of polymer-grafted lipid membranes. *Biochim Biophys Acta* 1108:40-48.
49. Branca C, Magaz S, Maisano G, Migliardo F, Migliardo P, Romeo G 2002. Hydration Study of PEG/Water Mixtures by Quasi Elastic Light Scattering, Acoustic and Rheological Measurements. *J Phys Chem B* 106:10272-10276.
50. Choi YK, Bae YH, Kim SW 1998. Star-Shaped Poly(ether-ester) Block Copolymers: Synthesis, Characterization, and Their Physical Properties *Macromolecules* 31:8766-8774.
51. Maarel JRCVD. 2007. Introduction To Biopolymer Physics. ed., Singapore: World Scientific Company. p Chapter 2.
52. Devanand K, Selser JC 1991. Asymptotic Behavior and Long-Range Interactions in Aqueous Solution of Poly(ethylene oxide). *Macromolecules* 24:5941-5947.
53. deGennes PG 1980. Conformations of Polymers Attached to an Interface. *Macromolecules* 13:1069-1075.
54. Torchilin VP, Papisov MI 1994. Why do polyethylene glycol-coated liposomes circulate so long? *J Liposome Research* 4:725-739.
55. Hyun H, Cho JS, Kim BS, Lee JW, Kim MS, Khang G, Park K, Lee HB 2008. Comparison of micelles formed by amphiphilic star block copolymers prepared in the presence of a nonmetallic monomer activator. *J Polymer Science: Part A: Polymer Chemistry* 46:2084-2096.
56. Toncheva V, Schacht E, Ng SY, Barr J, Heller J 2003. Use of Block Copolymers of Poly(Ortho Esters) and Poly (Ethylene Glycol) Micellar Carriers as Potential Tumour Targeting Systems. *J Drug Targeting* 11:345-353.
57. Doronin K, Shashkova EV, May SM, Hofherr SE, Barry MA 2009. Chemical Modification with High Molecular Weight Polyethylene Glycol Reduces Transduction of Hepatocytes and Increases Efficacy of Intravenously Delivered Oncolytic Adenovirus. *Human Gene Therapy* 20:1-14.
58. López-Esparza R, Guedeau-Boudeville M-A, Gambina Y, Rodríguez-Beas C, Maldonado A, Urbach W 2006. Interaction between poly(ethylene glycol) and two surfactants investigated by diffusion coefficient measurements. *J Colloid and Interface Sci* 300:105-110.
59. Charifson PS, Hiskey RG, Pedersen LG 1990. Construction and molecular modeling of phospholipid surfaces. *J Comp Chem* 11:1181-1186.
60. Flory PJ. 1953. Principles of Polymer Chemistry. ed., Ithaca, NY: Cornell University Press. p Chapter 7.
61. Ding WL, S.; Lin, J.; Zhang, L. 2008. Effect of Chain Conformational Change on Micelle Structures: Experimental Studies and Molecular Dynamics Simulations. *J Phys Chem B* 112:776-783.
62. Sigma-Aldrich, date of access: May 2009, <http://www.sigmaaldrich.com>
63. Koenig JL, Angood AC 1970. Raman Spectra of Poly(ethylene Glycols) in Solution. *Journal of Polymer Science Part A-2-Polymer Physics* 8:1787-1796.

Tables

Table 1: Composition of the [MePEG_x-*b*-PCL_y]₆ star copolymer systems used in the molecular dynamics simulations.

	y	1	2	3	4	6	9	18
x	MW _{PCL}	114	228	342	456	684	1026	1938
	MW _{PEG}							
6	279	71 0.1 5.47 5194						
12	543		70 8.5 5.93 6566					
19	851		79 5.0 7.04 11053	71 5.3 6.93 10482				
27	1203		84 3.5 7.96 16021	78 3.3 8.07 16634	73 3.7 7.81 15023			
38	1687			83 3.2 8.0 17412	79 3.5 7.96 15778	71 3.6 7.90 15335	62 3.2 8.23 17365	
113	4987							72 5.3 15.02 108338

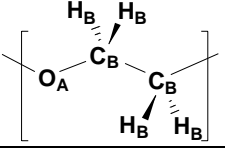
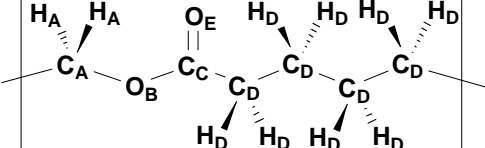
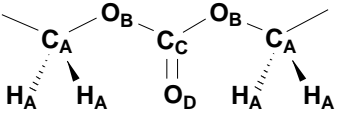
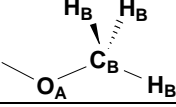
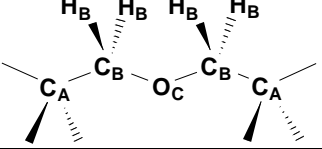
x and y are the number of repeat units in PEG and PCL blocks, respectively, in each arm of [MePEG_x-*b*-PCL_y]₆. MW_{PEG} and MW_{PCL} are the MW of PEG and PCL excluding the MW of initiator (248 g/mol⁻¹) per arm, respectively, expressed in g/mol⁻¹. Values in each box of the columns correspond in vertical order to the following: the PEG weight fraction (wt %), the concentration of star copolymer in water expressed in mol.mL⁻¹, the size of the cubic box expressed in nm³ and the number of water molecules

Table 2: Parameters for the description of the CH₂OCOOCH₂ fragment.

Atom types				Mass (g mol ⁻¹)	Charge (e)	σ (nm)	ε (kJmol ⁻¹)
O _D				15.99940	-0.500	0.296000	0.878640
O _B				15.99940	-0.450	0.300000	0.711280
C _C				12.01100	0.860	0.375000	0.439320
C _A				12.01100	0.210	0.350000	0.276144
Bond types				Bond length (nm)	Bond stretching (kJmol ⁻¹ nm ⁻²)		
O _D	C _C			0.12169	381999.0		
C _C	O _B			0.13279	220497.0		
O _B	C _A			0.14487	141001.0		
H _A	C _A			0.10900	284512.0		
Angle types ^a				Angle (Å)	(kJmol ⁻¹ rad ⁻²)		
O _B	C _C	O _B		110.4	429.2784		
O _D	C _C	O _B		124.8	430.5336		
C _C	O _B	C _A		119.2	348.1088		
O _B	C _A	H _A		109.5	292.880		
H _A	C _A	H _A		107.800	276.144		
C _D	C _C	O _D		125.200	669.440		
Dihedral Angle ^b				C ₁ (kJ mol ⁻¹)	C ₂ (kJmol ⁻¹)	C ₃ (kJmol ⁻¹)	C ₄ (kJmol ⁻¹)
C _A	O _B	C1	O _D	21.43881	0.00000	21.43881	0.00000
C _A	O _B	C1	O _B	16.15810	1.683820	-14.7337	-3.10824
H _A	C _A	O _B	C1	0.41421	1.24265	0.00000	-1.65686

(a) The H_AC_AH_A angle type was obtained from the standard OPLS-AA of alkanes; The C_DC_CO_D angle was adapted from Charifson *et. al.* study.⁵⁹ (b) Dihedral angle constants C₅ and C₆ = 0.00000. All other parameters were adapted from Okada *et. al.* study.¹⁹

Table 3: Charge assignments for the [MePEG_x-*b*-PCL_y]₆ star copolymer.

Residue of [MePEG _x - <i>b</i> -PCL _y] ₆	Atoms	Charge (e)
Poly(ethylene glycol) (PEG)		
	O _A	-0.400
	C _B	0.140
	H _B	0.030
Polycaprolactone (PCL)		
	C _A	0.190
	H _A	0.030
	O _B	-0.330
	C _C	0.510
	C _D	-0.120
	O _E	-0.430
	H _D	0.060
Connection Fragment: CH ₂ OCOOCH ₂		
	C _A	0.253
	O _B	-0.460 ^a
	C _C	0.799
	O _D	-0.505
	H _A	0.030
Terminal group: CH ₂ OCH ₃		
	O _A	-0.400
	C _B	0.110
	H _B	0.030
Central Connection: (CCH ₂ O) ₂		
	C _A	0.000
	C _B	0.140
	O _C	-0.400
	H _B	0.030

a. value adapted from ref. 19

Table 4: Properties of PCL core following molecular dynamics simulation for 200 ns.

x	y	R_{g_core} (nm)	R_{g_star} (nm)	W_{PCL}	Asphericity	SAS_{PCL} (nm ²)	f_{PCL}
6	1	0.58 ± 0.02	0.94 ± 0.03	59 ± 3	0.028 ± 0.009	6.3 ± 0.3	0.55
12	2	0.73 ± 0.04	1.18 ± 0.05	80 ± 6	0.025 ± 0.011	8.5 ± 0.6	0.50
19	2	0.74 ± 0.05	1.35 ± 0.06	68 ± 6	0.042 ± 0.024	7.3 ± 0.6	0.43
27	2	0.77 ± 0.03	1.50 ± 0.09	64 ± 9	0.049 ± 0.021	6.8 ± 0.9	0.36
19	3	0.82 ± 0.04	1.32 ± 0.06	89 ± 7	0.031 ± 0.011	9.5 ± 0.7	0.44
27	3	0.84 ± 0.03	1.49 ± 0.07	81 ± 8	0.020 ± 0.008	8.6 ± 0.9	0.35
38	3	0.81 ± 0.04	1.70 ± 0.09	64 ± 8	0.030 ± 0.013	6.8 ± 0.8	0.32
27	4	0.87 ± 0.03	1.49 ± 0.07	91 ± 7	0.029 ± 0.013	9.7 ± 0.7	0.38
38	4	0.88 ± 0.03	1.65 ± 0.09	78 ± 11	0.023 ± 0.010	8.3 ± 1.1	0.32
38	6	0.99 ± 0.03	1.60 ± 0.06	105 ± 10	0.022 ± 0.009	11.2 ± 1.1	0.32
38	9	1.08 ± 0.02	1.61 ± 0.02	142 ± 11	0.008 ± 0.001	15.1 ± 1.2	0.35
113	18	1.35 ± 0.02	2.41 ± 0.16	157 ± 11	0.009 ± 0.005	16.7 ± 1.1	0.23

x and y are the number of repeat units in the PEG and PCL blocks, respectively, of each arm in the [MePEG_x-*b*-PCL_y]₆. R_{g_core} R_{g_star} are the radius of gyration of the polycaprolactone (PCL) core (PCL and dipentaerythriol initiator) and star copolymer, respectively; W_{PCL} is the number of water molecules within 0.35 nm of the PCL. SAS_{PCL} is the solvent accessible surface area of PCL. f_{PCL} is the ratio of W_{PCL} to W_{totPCL} and represents the fraction of the hydrophobic core exposed to water, *i.e.* $f_{PCL} = W_{PCL}/W_{totPCL}$.

Table 5: Properties of the PEG blocks and star copolymers following molecular dynamics simulation for 200 ns, in comparison to calculated Flory radius and area protected by PEG based on previously established models.

x	y	R_{g_PEG} (nm)	W_{PEG} ^a	SAS_{PEG} (nm ²)	$S_{PEG-PCL}$ (nm ²) ^b	R_{gF_PEG} (nm) ^c	$S_{random-coil}$ (nm ²) ^d
6	1	0.43 ± 0.02	217 ± 7 (5.4)	20.6 ± 0.7	4.99	0.33	3.0
12	2	0.63 ± 0.03	361 ± 13 (4.7)	36.1 ± 1.3	8.4	0.49	4.9
19	2	0.80 ± 0.04	510 ± 25 (4.3)	52.1 ± 2.5	9.7	0.65	8.4
19	3	0.80 ± 0.05	496 ± 26 (4.2)	50.6 ± 2.6	12.9		
27	2	0.97 ± 0.05	661 ± 29 (4.0)	68.1 ± 3.0	11.9	0.79	12.8
27	3	0.93 ± 0.06	661 ± 29 (3.9)	68.0 ± 3.0	15.8		
27	4	0.96 ± 0.06	668 ± 41 (4.0)	68.9 ± 4.1	15.9		
38	3	1.08 ± 0.07	906 ± 42 (3.9)	94.3 ± 4.4	14.6	0.97	19.4
38	4	1.09 ± 0.07	864 ± 47 (3.7)	90.1 ± 4.9	17.8		
38	6	1.10 ± 0.06	854 ± 44 (3.7)	89.1 ± 4.5	23.2		
38	9	1.15 ± 0.07	866 ± 31 (3.7)	90.1 ± 3.2	28.6		
113	18	1.68 ± 0.07	2283 ± 125 (3.2)	242.0 ± 13.1	55.7	1.84	71.6

x and y are the number of repeat units in the PEG and PCL blocks, respectively, for each arm of [MePEG_x-b-PCL_y]₆. R_{g_PEG} is the radius of gyration of the poly(ethylene glycol) (PEG). W_{PEG} is the number of water molecules within 0.35 nm of the PEG blocks. SAS_{PEG} is the total solvent accessible surface area of PEG; (a) Values in parentheses are number of water molecules per repeat unit; (b) The surface area of PCL protected by PEG calculated based on MD simulation: $S_{PEG-PCL} = S_{PCL} - SAS_{PCL}$; (c) R_{gF_PEG} is the radius of gyration for PEG calculated based on Flory's model⁶⁰; (d) The area protected by PEG is calculated based on a theoretical model described elsewhere assuming a random coil conformation for PEG,⁵⁴ $S_{random-coil} = \pi \times R_F^2$ where R_F is the Flory radius of PEG (see supplemental information).

Figures

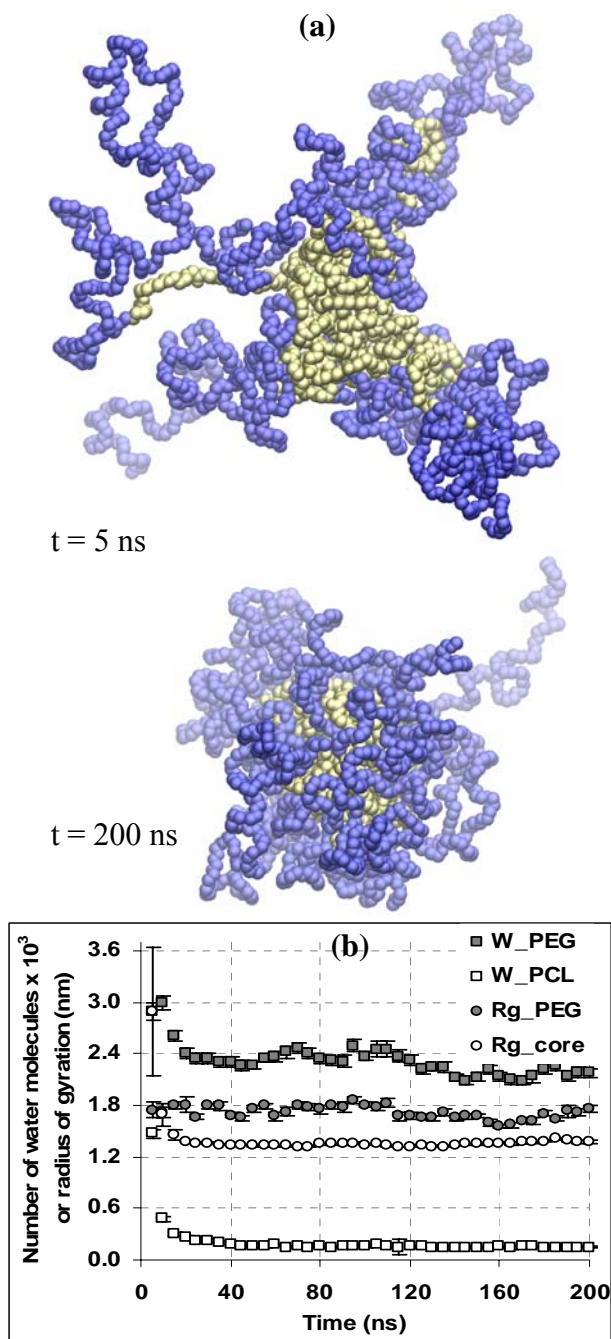


Figure 1: (a) Snapshots of conformations of [MePEG₁₁₃-b-PCL₁₈]₆ at 5 ns and 200 ns. The PCL core and PEG blocks are shown in yellow and blue, respectively. Bulk water and hydrogen atoms are omitted for clarity. (b) Radius of gyration of PCL core (○) or PEG blocks (●), hydration of PCL core (□) and PEG blocks (■) of [MePEG₁₁₃-b-PCL₁₈]₆ as a function of simulation time.

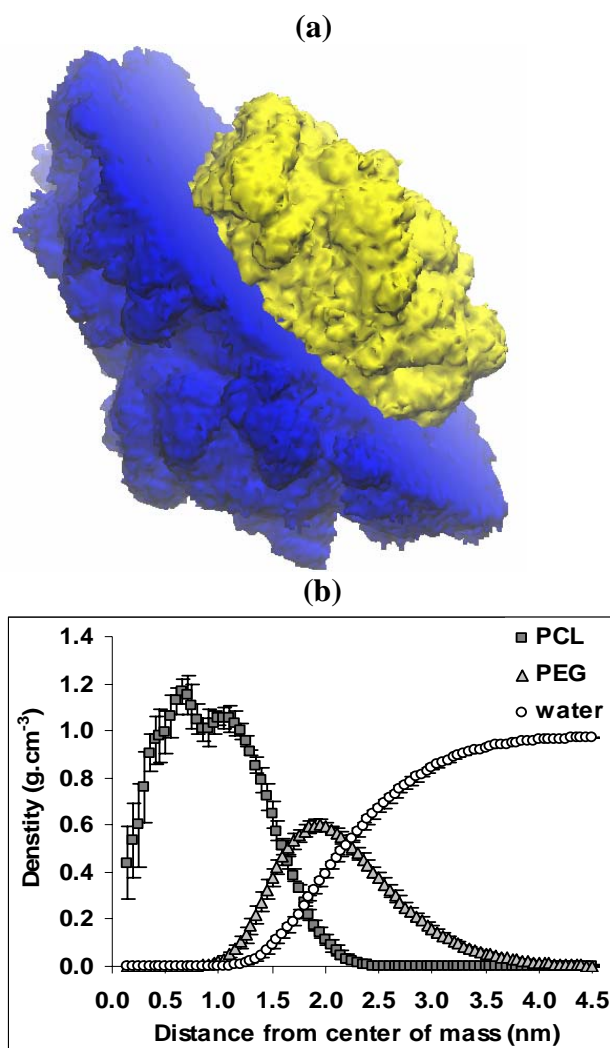


Figure 2: Spatial distribution of the $[\text{MePEG}_{113}\text{-}b\text{-PCL}_{18}]_6$ (a) Cross section through a randomly selected snapshot from the simulation of the poly(ethylene glycol) (PEG) corona (blue) and the polycaprolactone (PCL) core (yellow) (b) Density profile of PCL core (■), PEG blocks (▲), and water (○) as a function of distance from the center of mass of the PCL core averaged over the last 160 ns of molecular dynamics simulation.

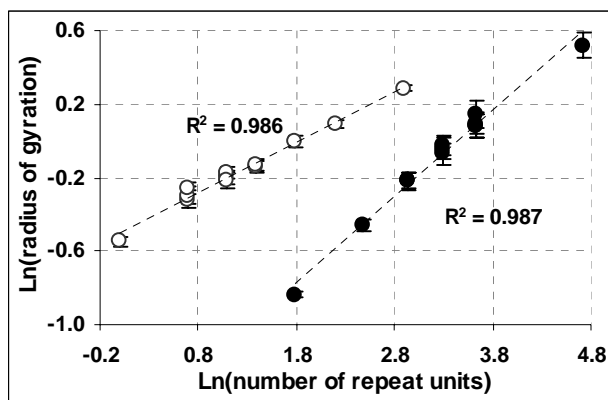
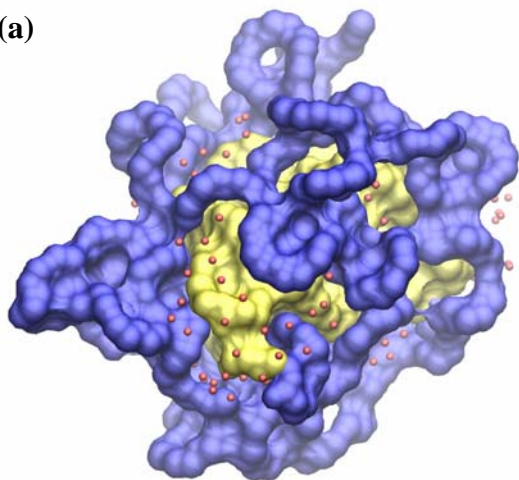


Figure 3: The mean radius of gyration of the hydrophobic polycaprolactone (PCL) blocks versus the degree of polymerization of PCL (\circ) and poly(ethylene glycol) (PEG) blocks versus the degree of polymerization of PEG (\bullet) with double-logarithmic scales for $[\text{MePEG}_y\text{-}b\text{-PCL}_x]_6$ star copolymers. Data were evaluated using the trajectory from the last 160 ns of the molecular dynamics simulations. The dashed lines are the linear fit functions.

(a)



(b)

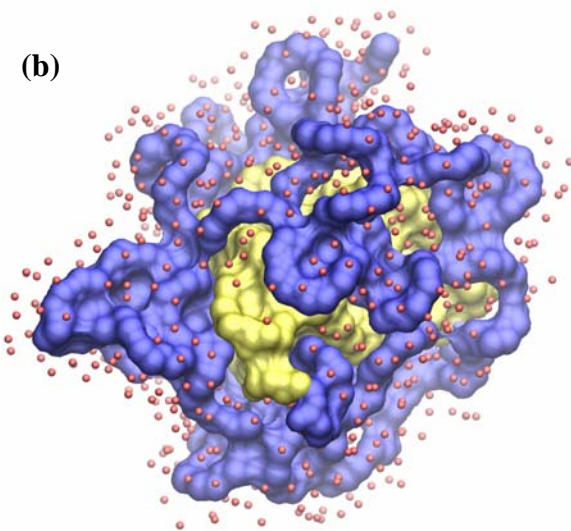


Figure 4: Snapshot of the [MePEG₁₁₃-*b*-PCL₁₈]₆ SCP highlighting the interaction of water molecules within 3.5 Å of **(a)** polycaprolactone (PCL) (yellow) and **(b)** poly(ethylene glycol) (PEG) (blue) residues at 200 ns. Bulk water and hydrogen atoms are omitted for clarity.

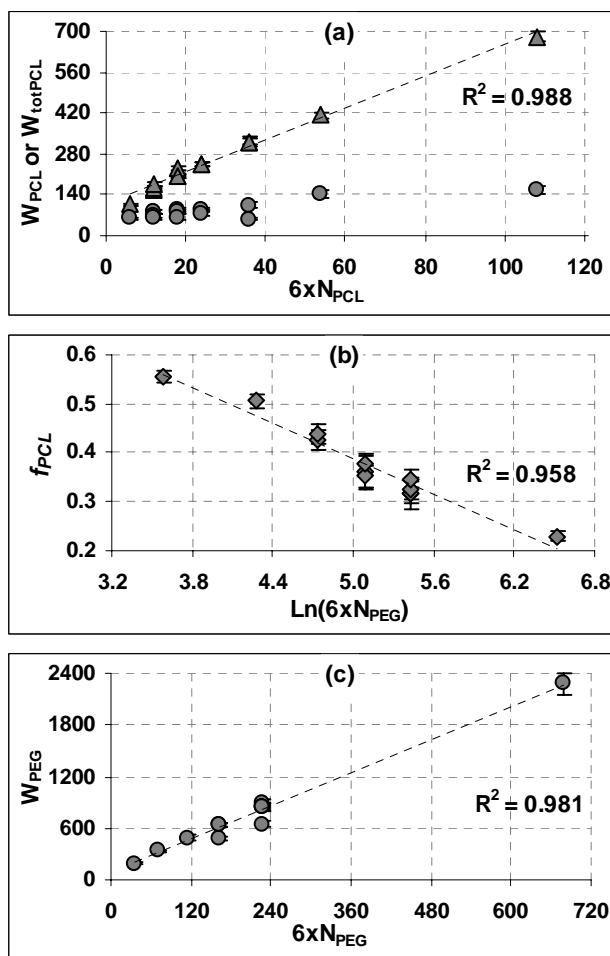


Figure 5: Hydration of various star copolymers, obtained by calculating the number of water molecules within 3.5 Å of the polymers. (a) Hydration of polycaprolactone (PCL) core assuming zero protection by PEG (▲) and with protection by PEG (●) (b) Fraction of PCL interacting with water (c) Hydration of poly(ethylene glycol) (PEG) corona. Data were evaluated using the trajectory from the last 160 ns of the molecular dynamics simulation. N_{PCL} and N_{PEG} are the number of repeat units in the PCL and PEG, blocks, respectively, in each arm of the star copolymers. The dashed lines are the linear fit functions.

Supplemental Information

1. Asphericity of hydrophobic PCL core

Many studies have been put forth to measure the asphericity of a cluster or group.^{31,61} In this study, the asphericity of the hydrophobic PCL core was determined by employing a theoretical model that was established by Bruns and Carl as shown in Equation S1.³¹

$$\text{Asphericity} = 1 - 3 \left\langle \frac{x^2 y^2 + y^2 z^2 + z^2 x^2}{(x^2 + y^2 + z^2)^2} \right\rangle \quad \text{Eq. (S1)}$$

where x , y and z are axes for the principal moments, which were obtained from the radius of gyration of the components. An asphericity value of 0 is achieved for a perfect sphere. The asphericity of the core causes a broadened distribution of the PCL and PEG blocks as well as water (Figure S1). This broadening results in a significant overlap between the density distribution curves, although the PEG blocks do not penetrate into the collapsed hydrophobic PCL core of the SCPs, i.e. the PCL core excludes not only the water, but also the PEG blocks. As shown in Figure S1, the density of PCL ($N_{\text{PCL}} = 18$) that is obtained from the MD simulations is similar to the bulk density reported for PCL ($1.15 \text{ g}\cdot\text{cm}^{-3}$) of a similar MW.⁶²

2. End-to-End distance of PEG

As shown in Figure S2, for SCPs with shorter PEG chains, the distal end of all PEG blocks remained extended with median EED of $0.80 \pm 0.01 \text{ nm}$ ($N_{\text{PEG}} = 6$) and $1.05 \pm 0.01 \text{ nm}$ ($N_{\text{PEG}} = 12$). For SCPs with $N_{\text{PEG}} > 12$, the distal ends of the PEG blocks often extend away from the center of the hydrophobic core, and then curl back to form an expanded coil providing protection of the hydrophobic core (Figure S2). Furthermore, hydrogen-bond “bridges” between PEG arms or PEG repeat units were observed as shown in Figure S3.

3. Theoretical model for predicting the structural properties of PEG

Previously, Flory put forth the “random flight” model to predict the size of linear polymers in terms of the radius of gyration, R_g (the average root mean square distance of

a segment from the COM of the molecule).⁶² R_g is approximately proportional to $R/\sqrt{6}$, where R (i.e. the root mean square end-to-end distance) scales with the size of the monomer, a , and the degree of polymerization of the polymer to a power law (i.e. $R \approx aN^\alpha$).⁵¹⁶² In a theta solvent, the polymer behaves ideally and exists as a Gaussian coil with an α value of 0.5. In the poor solvent, polymer closely packed and has α value of $1/3$. and good solvent ($\alpha = 0.588$).⁵¹ In the good solvent, the radius of R is known as the Flory radius with a value of 0.588 ($R_F = aN^{3/5}$). In the current study, the size of the PEG chain can be expressed in terms of radius of gyration based on Flory's theory:

$$R_{gF_PEG} = \frac{a}{\sqrt{6}} N_{PEG}^\alpha \quad (S2)$$

where $a = 0.28$ nm for PEG.⁶³ According to de Gennes' definition of random coil conformation, at a low graft density, the linear polymer adopts a random coil conformation in the “mushroom regime” which is defined as a “half-sphere with a radius comparable to the R_F of a coil in a good solvent”.⁵³ Based on a model put forth by Torchilin and Papisov,⁵⁴ the surface area of PEG that can protect liposomes from water is proportional to the surface area of a hemisphere with a radius approximately equal to R_F , assumes a random coil conformation.⁵³ Accordingly, the surface area of the PCL core protected by the PEG blocks ($S_{\text{random-coil}}$) was calculated using Equation S3.

$$S_{\text{random-coil}} = \pi R_F^2; \quad \text{where } R_F = aN^{3/5} \quad (S3)$$

Supplemental Figures

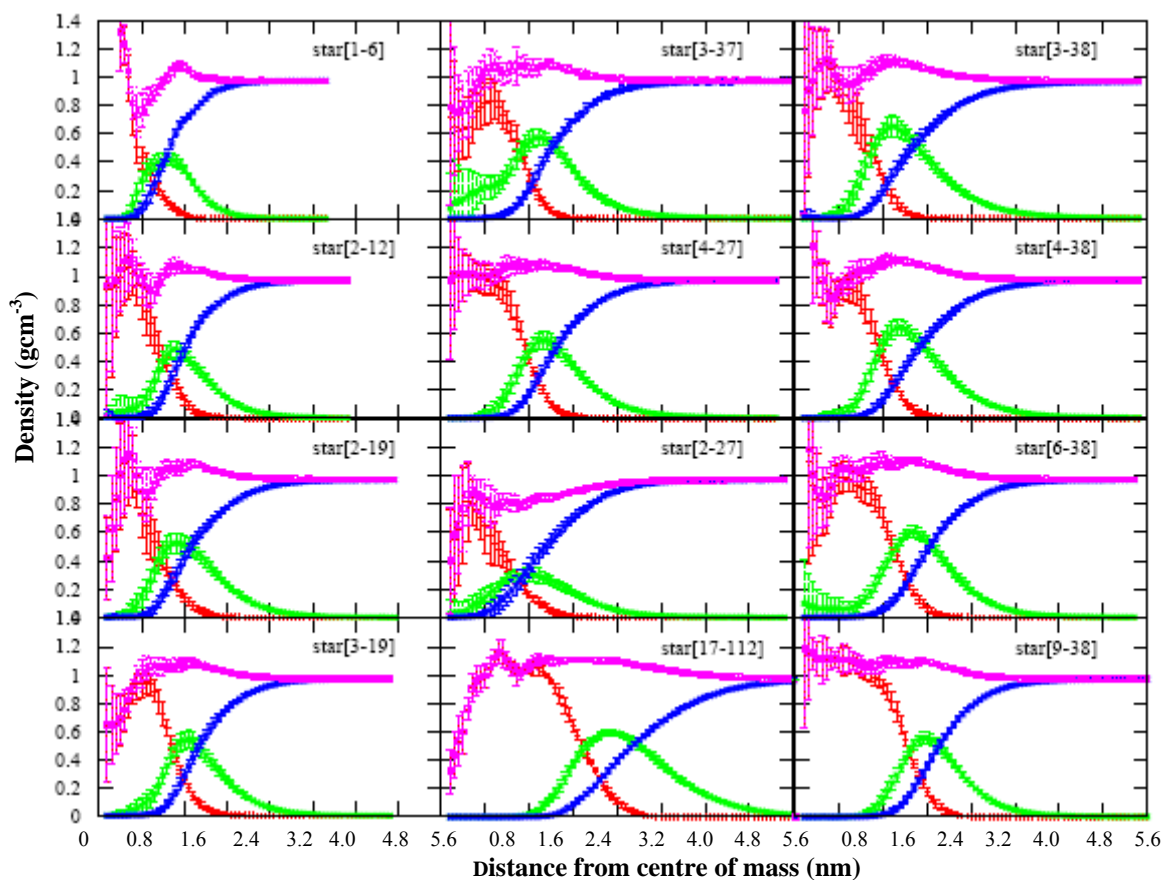


Figure S1: Density profiles of poly(ethylene glycol) (PEG) (\square), polycaprolactone (PCL) (\diamond), water (\blacksquare) and the whole system (\blacksquare) as a function of distance from the center of mass of the hydrophobic core, averaged over the last 160 ns.

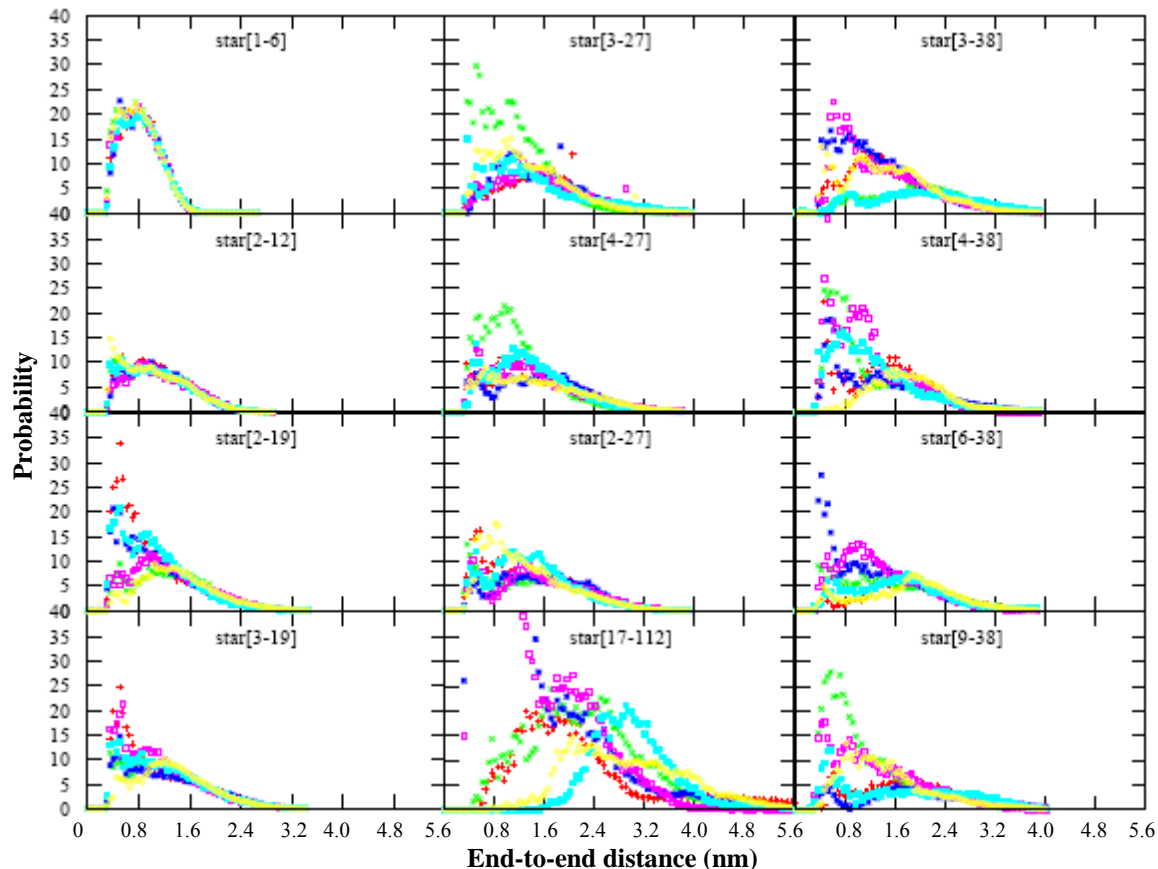


Figure S2: The end-to-end distance distribution of the PEG blocks for all [MePEG_x-*b*-PCL_y]₆ SCPs, averaged over the last 160 ns of molecular dynamics simulation.

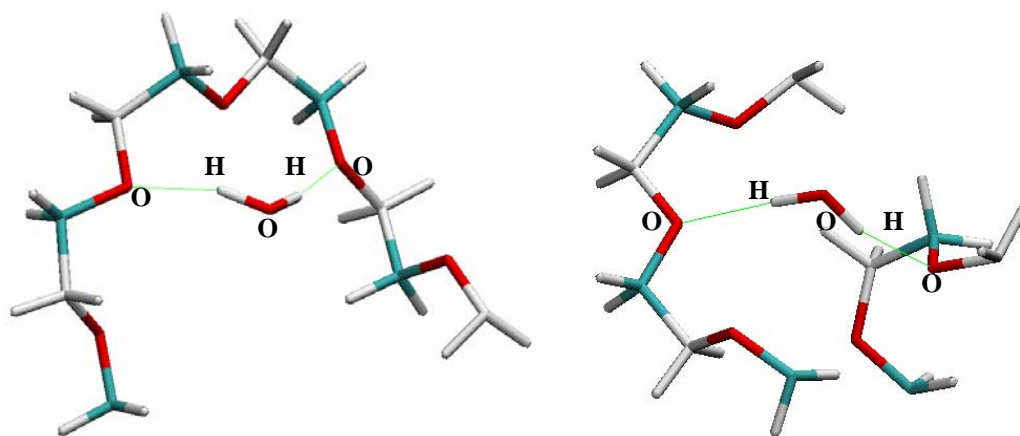


Figure S3: (a) Hydrogen bond (green line) formed between the hydrogen atom of a water molecule and the oxygen atoms of (a) PEG repeat units within the same PEG block or (b) “bridging” two PEG repeat units from different PEG blocks.